Processing and Properties of Modified Polyamide 66-Organoclay Nanocomposites

Miray Mert, Ulku Yilmazer

Chemical Engineering Department, Middle East Technical University, 06531 Ankara, Turkey

Received 9 March 2007; accepted 26 July 2007
DOI 10.1002/app.27974
Published online 17 March 2008 in Wiley InterScience (www.interscience.wiley.com).

ABSTRACT: Binary polyamide 66 nanocomposites containing 2 wt % organoclay, polyamide 66 blend containing 5 wt % impact modifier, and ternary polyamide 66 nanocomposites containing 2 wt % organoclay and 5 wt % impact modifier were prepared by melt compounding method. The effects of E-GMA and the types of the organoclays on the interaction between the organoclay and the polymer, dispersion of the organoclay, morphology, mechanical, flow, and thermal properties of the nanocomposites were investigated. Partial exfoliation and improved mechanical properties are observed for Cloisite® 15A and Cloisite® 25A nanocomposites. On the other hand, the organoclay was intercalated or in the form of tactoids in Cloisite® 30B nanocomposites. Components of the nanocomposites containing Cloisite® 15A and Cloisite® 25A were compounded in different addition orders. Mixing sequence of the components affected both the dispersion of the organoclay and the mechanical properties drastically. SEM analyses revealed that homogeneous dispersion of the organoclay results in a decrease in the domain sizes and promotes the improvements in the toughness of the materials. Melt viscosity was also found to have a profound effect on the dispersion of the organoclay according to MFI and XRD results. Crystallinity of the nanocomposites did not change significantly. It is only the type of the constituents and their addition order what dramatically influence the nanocomposite properties. © 2008 Wiley Periodicals, Inc. J Appl Polym Sci 108: 3890–3900, 2008

Key words: nanocomposite; polyamide 66; impact modifier; organoclay; melt compounding

INTRODUCTION

Polymer-clay nanocomposites have become one of the most prominent research areas in recent years. They are composed of nanoclay particles dispersed in a polymer matrix whose at least one dimension is in the nanometer range.[1] Nanocomposites can exhibit enhanced mechanical properties,[2–5] increased optical transparency,[1,6] improved gas barrier properties,[7,8] superior flame retardancy,[9,10] higher thermal stability,[11,12] and heat distortion temperature[13,14] at low clay loadings compared to conventional composites.

Layered silicates such as montmorillonite which is a structural group of 2 : 1 phyllosilicates and an undergroup of smectites can be used for the synthesis of polymer-clay nanocomposites.[15] The layer thickness of montmorillonites is around 1 nm and the lateral dimensions range from 30 nm to several microns.[16] Hydrophobic silicate surface is not compatible with the hydrophilic polymer matrices and it has to be converted into an organophilic nature to facilitate its miscibility with the polymer. This can be achieved by the ion exchange reactions of the cations in the intergallery of the clay with the cationic surfactants including alkylammonium or alkylphosphonium cations.[17] The cation exchange capacity changes between 80 and 150 mequiv./100 g for smectites.[15]

Nanocomposites can be processed by many different methods such as solution polymerization, *in situ* polymerization, and melt compounding.[1] Although nanocomposites of polymers having a nonpolar chemical structure can more easily be synthesized by solution and *in situ* polymerization, melt compounding method is more advantageous in terms of its compatibility with the industrial processing techniques and elimination of the use of organic solvents from the reaction medium.[17] However, the type of the extruder and screws, residence time, shear intensity, chemical compatibility, and type of the constituents all play an important role on the delamination of the organoclay in the polymer matrix in melt compounding method.[18]

The presence of polar groups both in the chemical structure of the polymer and the organic modifier is of utmost importance for homogeneous dispersion of the organoclay.[19] Some other functional groups can be incorporated by using impact modifiers that also function as compatibilizers to increase the binding forces between the clay surface and the polymer, and result in an increase in the toughness of nanocomposites.[20] High aspect ratio of the organoclays creates a

Correspondence to: U. Yilmazer (yilmazer@metu.edu.tr).
Contract grant sponsor: The Scientific and Technological Research Council of Turkey (TUBITAK); contract grant number: 104M415.

large contact area, and stiffens the matrix.[21] However, high elongation at break values diminish upon addition of the reinforcement phase since inorganic silicate particles cannot be strained by external stresses. Elastomeric materials can be incorporated into the matrix to compensate for the decrease in ductility, since they can act as stress concentrators and intensify the energy absorption during crack formation.[22]

The properties of the polymer matrix as well as the organoclay and the impact modifier properties are extremely significant in nanocomposite preparation. Fatigue resistance, resistance to oils and solvents, low friction, abrasion resistance, stability at high temperature, fire resistance, drawability, creep resistance, good appearance, and good molding economics constitute the important commercial properties of PA 66 whose polar chemical structure makes it suitable for nanocomposite production especially by melt compounding method. In spite of all these advantages and its high resistance to crack initiation, PA 66 is somewhat less resistant to crack propagation.[23] Therefore, it is customary to blend it with elastomeric materials to obtain improved impact strength.

This study is carried out to investigate the effect of the addition of Lotader® 8840 (E-GMA), a random copolymer of ethylene and glycidyl methacrylate, on the morphology and mechanical, thermal, and flow properties of polyamide 66 blend and polyamide 66 nanocomposites containing three different types of organoclays including Cloisite® 15A, Cloisite® 25A, and Cloisite® 30B. The mixing sequences of the components were also varied.

X-ray diffraction (XRD), scanning electron microscopy (SEM), differential scanning calorimetry (DSC), melt flow index (MFI) analyses, impact and tensile tests were conducted to observe the variations in the properties of the nanocomposites. The changes in the domain sizes of the impact modifier and dispersion of the organoclay are correlated with the enhancements in the toughness.

EXPERIMENTAL

Materials

Polyamide 66 (Bergamid A65) was obtained commercially from Polyone Company (Istanbul, Turkey). Impact modifier, Lotader® 8840, a random copolymer of ethylene (E) and glycidyl methacrylate (GMA), was supplied by Arkema Chemicals (France). The glycidyl methacrylate content of the elastomeric material is 8 wt %.

Three montmorillonite clays including Cloisite® 15A, Cloisite® 25A, and Cloisite® 30B were purchased from Southern Clay Products (Gonzales, TX). Cloisite® 15A has a cation exchange capacity of 125 mequiv./100 g clay and it is treated with dimethyl, dehydrogenated tallow quaternary ammonium chloride. Cloisite® 25A is ion-exchanged with dimethyl, hydrogenated tallow, 2-ethylhexyl quaternary ammonium cation, and methyl sulfate anion at a concentration of 95 mequiv./100 g clay. The alkyl ammonium surfactant of Cloisite® 30B with a cation exchange capacity of 90 mequiv./100 g is methyl, tallow, bis-2-hydroxyethyl quaternary ammonium chloride. Molecular structures of the organic modifiers are given in Figure 1.

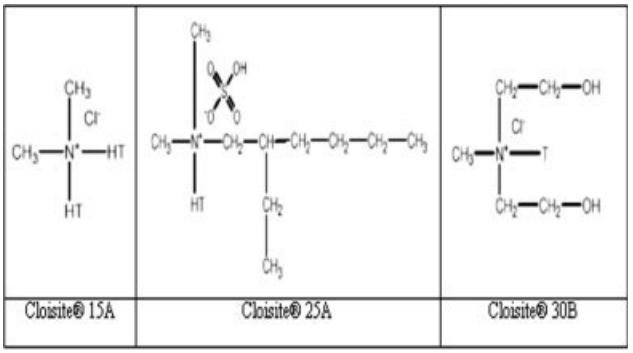

Figure 1 Molecular structures of the organic modifiers.

Melt compounding

Binary polyamide 66 nanocomposites (2 wt % organoclay), ternary polyamide 66 nanocomposites (2 wt % organoclay and 5 wt % impact modifier), and polyamide 66 blend (5 wt % impact modifier) were prepared using a Thermoprism TSE 16 TC, corotating, intermeshing twin-screw extruder (D = 16 mm, L = 384 mm). Compounding was carried out at 200 rpm and 25 g/min feed rate. Temperature profile of the barrel was set to 260-275-275-275-280°C from hopper to die. All polyamide 66 containing materials were dried at 100°C *in vacuo* for 24 h prior to each processing step. Organoclays and the impact modifier were also dried for 12 h under vacuum at 80 and 40°C, respectively.

All the combinations were extruded twice for obtaining homogeneous organoclay dispersion. Injection molding of the specimens was carried out immediately following the second extrusion step using DSM Xplore micro injection molding equipment at a barrel temperature of 275°C and mold temperature of 30°C. The specimens were sealed in polyethylene bags soon after the injection molding and kept in desiccators for at least 24 h prior to testing.

X-ray diffraction

XRD was performed by RIGAKU D/MAX 2200/PC X-ray diffractometer at 40 kV and 40 mA, using a monochromatic Cu Kα radiation source (λ = 1.5418). XRD diffraction patterns were recorded with a step size of 0.01° from 2θ = 1° to 10° at 1°/min scan rate.

The interlayer spacings of the organoclays (d_{001} reflection) were calculated from the peak positions according to Bragg's equation.

Scanning electron microscopy

Surfaces of impact-fractured specimens coated with gold were examined to observe the failure mechanisms by SEM (JEOL JSM-6400). Elastomeric phase was extracted by etching the samples in boiling xylene for 6 h. SEM micrographs were taken at 3500 × magnification and the elastomeric domain sizes of all the combinations were calculated by the image analysis program Image J for a number of elastomeric domains that range between 100 and 250.

Mechanical testing

Tensile tests were carried out according to ISO 527 using Lloyd LR 5K Universal Testing Machine at a strain rate of 0.1/min. Notched Charpy impact tests of one sided notched specimens with dimensions of 80 mm × 10 mm × 4 mm were conducted by a pendulum Ceast Resil Impactor according to ISO 179. The tests were performed at 23°C and the reported results are the averages of five specimens.

Melt flow index

MFI tests were performed according to ISO 1133 using Omega Melt Flow Indexer at 275°C under a load of 0.325 kg. The amount of the material flowing through the capillary of the instrument in 10 min was calculated by taking the average of five measurements.

Differential scanning calorimetry

Ten milligram samples which were cut from dry tensile bars were heated from 25 to 280°C with a heating rate of 5°C/min in General V4.1.C DuPont 2000. Indium was used as a calibration standard. Percent crystallinity was determined from the ratio of the heat of fusion of the specimen and the heat of fusion of 100% crystalline PA 66 (206 J/g).[24]

RESULTS AND DISCUSSION

XRD analysis

XRD pattern of pure Cloisite® 15A and all the mixing sequences of binary and ternary polyamide 66 nanocomposites containing Cloisite® 15A is shown in Figure 2. The mixing sequence in which the organoclay and the impact modifier were blended first and compounded with the polymer in the second extrusion step is abbreviated as CI-P. In the other

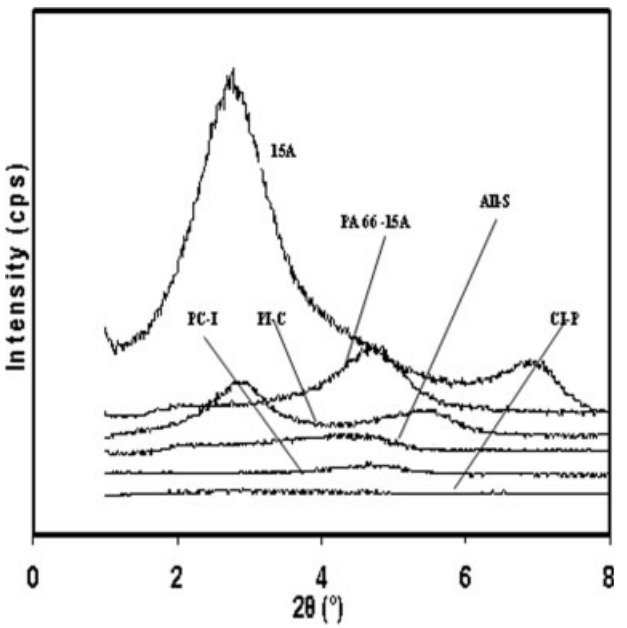

Figure 2 XRD patterns of PA 66-Cloisite® 15A-Lotader® AX8840 mixing sequences.

mixing sequences, the polymer was either melt blended with the organoclay (PC-I) or with the impact modifier first (PI-C). The second extrusion step involves the use of impact modifier with polymer-organoclay combination in PC-I mixing sequence or organoclay with polymer-impact modifier combination in PI-C mixing sequence. All-S denotes the mixing sequence in which all the components were compounded simultaneously first. The combination of the constituents of All-S mixing sequence was subjected to extrusion once more.

Bragg's equation was used to determine the changes in *d*-spacings of the organoclays given in Table I. It can be inferred that disappearance of the peak indicates complete delamination of the organoclay in the polymer matrix, while a shift in the position of the peak to lower angles is a sign of the intercalated structure.[25] The presence of more than one peak on XRD pattern of Cloisite® 15A can be attributed to a second silicate layer or a portion of the smectite clay whose inorganic cations were not fully replaced by the organic ions.[26,27] The first basal spacing is indicative of the changes in the structure. Cloisite® 15A was partially exfoliated in the polymer matrix in its binary nanocomposites and All-S mixing sequences. In addition to the increase in the *d*-spacing, the intensity of both the peaks decreased to a greater extent when compared with the pure organoclay. Reduction in the intensity of the peaks manifests that the platelet agglomerates were broken down into tactoids and the amount of intercalated clay decreased in the polymer matrix leading to a partially exfoliated structure.[28] The same thing is

TABLE I
XRD Results

Components	*d*-spacing (d_{001}) (Å)
Organoclays	
Cloisite®15A	32.0
Cloisite®25A	18.0
Cloisite®30B	18.0
PA 66 binary nanocomposites	
PA 66-15A	46.3
PA 66-25A	63.1
PA 66-30B	18.6
PA 66 ternary nanocomposites	
(PA 66-15A-8840)-(All-S)	44.2
(PA 66-25A-8840)-(All-S)	52.9
(PA 66-30B-8840)-(All-S)	40.5
Mixing sequences of PA 66 ternary nanocomposites	
(15A/8840)-PA 66-(CI-P)	33.3
(PA 66/15A)-8840-(PC-I)	–
(PA 66/8840)-15A-(PI-C)	31.7
(25A/8840)-PA 66-(CI-P)	–
(PA 66/25A)-8840-(PC-I)	53.2
(PA 66/8840)-25A-(PI-C)	43.7

also valid for Cloisite® 25A nanocomposites wherein the clay was mostly intercalated as it can be seen in Figure 3. On the other hand, Cloisite® 30B was not as well dispersed in the polymer matrix as the other organoclays. It can obviously be seen from XRD patterns of Cloisite® 30B nanocomposites in Figure 4 that the intercalated region is smaller in size since the characteristic peak of the organoclay is higher in intensity than the small shoulder at lower angles. This means that complete separation of the clay platelets could not be achieved. Besides the presence of

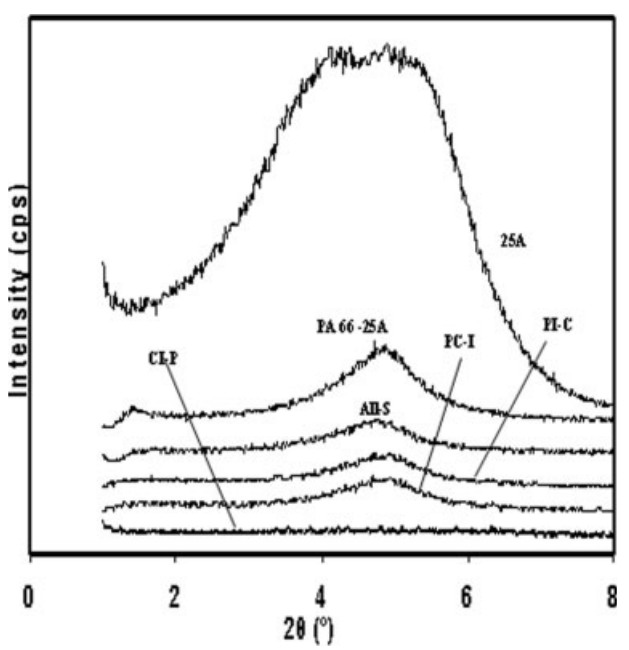

Figure 3 XRD patterns of PA 66-Cloisite® 25A-Lotader® AX8840 mixing sequences.

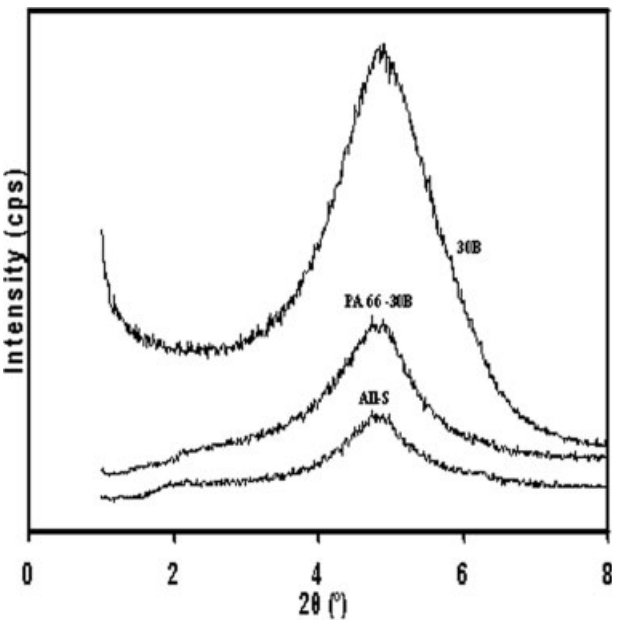

Figure 4 XRD patterns of PA 66-Cloisite® 30B nanocomposites.

a few exfoliated structures in Cloisite® 30B nanocomposites, most of the organoclay is intercalated or in the form of tactoids.[22] Therefore, the addition orders varied for Cloisite® 15A and Cloisite® 25A nanocomposites. Although the most polar organic modifier belongs to Cloisite 30B, the interactions of the hydroxyl groups within the organic modifier's structure and with the oxygen groups located on the clay surface made it adopt a structure with high packing density, and prevented formation of the binding forces between the clay surface and the polymer.[29] It is also emphasized that the interaction between clay and organic modifier is higher than the interaction between polymer and clay.[30] Besides the fact that organic modifier polarity plays an important role in binding the polymer chains to the clay surface at the first step, exfoliation level is also largely affected by platelet-modifier and modifier-polymer interactions, the amount of platelet–platelet separation, stability of the organic modifier, and packing density.[19] On the other hand, extruding the polymer matrix twice may have eliminated the effect of the repulsive nonpolar interactions between the polymer matrix and the hydrogenated tails of the organic modifier of both Cloisite® 15A and Cloisite® 25A, and aid in delamination of the organoclays.

PC-I and CI-P mixing sequences of Cloisite® 15A and Cloisite® 25A nanocomposites showed better dispersion in comparison with PI-C mixing sequences. Melt viscosity is expected to be higher for PI-C and CI-P mixing sequences, and promote delamination of the organoclay. However, the organoclay undergoes only one extrusion step in PI-C mixing

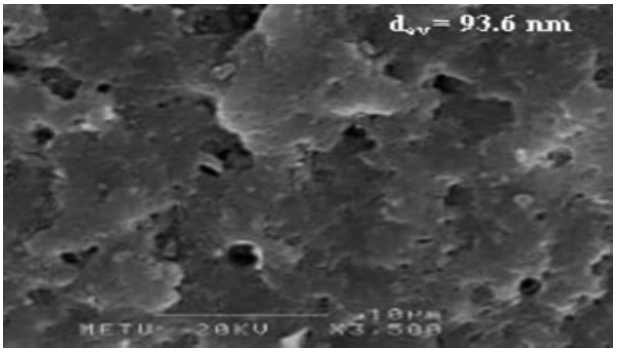

Figure 5 SEM micrograph of PA 66-Lotader® AX8840 blend.

sequence, and the shear intensity applied in a single extrusion step was insufficient for organoclay dispersion. On the other hand, a more uniform dispersion is attained for CI-P and PC-I mixing sequences where the clay was subjected to extrusion twice. Complete exfoliation is observed in (25A/8840)-PA 66-(CI-P) mixing sequence.

It can be concluded that organoclay exfoliation is not solely affected by organic modifier polarity, although it is a significant factor in forming the interactions with the clay surface in the first step. Packing density of the organic modifier, arising from the interactions of the polar groups of the organic modifier with the polar groups in its structure and the clay surface, should allow passage of the polymer chains to interact with the clay surface. The shear intensity also has to be sufficient to yield higher dispersive forces for homogeneous dispersion of the organoclay since organoclay delamination is a function of the shear intensity, structural and thermal properties of the organic modifier and the interactions taking place between the organic modifier, clay layers, and the polymer.

SEM analysis

SEM analysis was conducted to examine the impact fractured surfaces of polyamide 66 nanocomposites and polyamide 66-8840 blend, and calculate the domain sizes by Image analysis program, Image J. The domain sizes of (PA 66-30B-8840)-(All-S) could not be calculated since both the number and the size of the elastomer domains is not at a sufficient level for domain size analysis. SEM micrographs of the blend and Cloisite® 15A, Cloisite® 25A, and Cloisite® 30B nanocomposites are presented with the average domain sizes in Figures 5–8, respectively.

Presence of functional groups on the organic modifier, polymer or impact modifier increases the adhesion between the constituents, since surface tension is lowered and the interface is immobilized as chemical reactions are formed at the interface. Otherwise, stress transfer cannot be achieved between the phases leading to failure of the material as the physical interactions are overcome.[22]

GMA group of the impact modifier is expected to react with the acid and amine ends of polyamide 66.[31] The possibility of the reactions that can take place between all the components also increases owing to the presence of extra functional groups incorporated into the reaction medium by the impact modifier. Impact modifier acts both as a compatibilizer and a toughening agent here. Bonding at the interface, elastomer domain sizes, and interdomain distances all influence toughness of the materials.

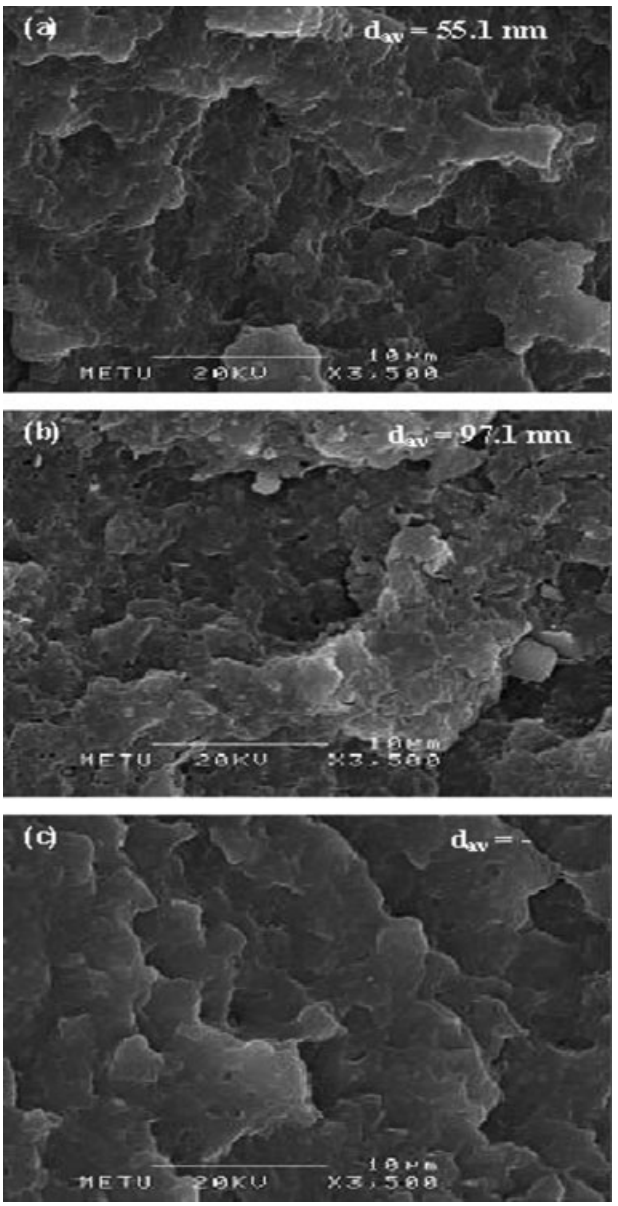

Figure 6 SEM micrographs of PA 66-Organoclay-Lotader® AX8840 All-S ternary nanocomposites: (a) Cloisite® 15A (3500×); (b) Cloisite® 25A (3500×); (c) Cloisite® 30B (3500×).

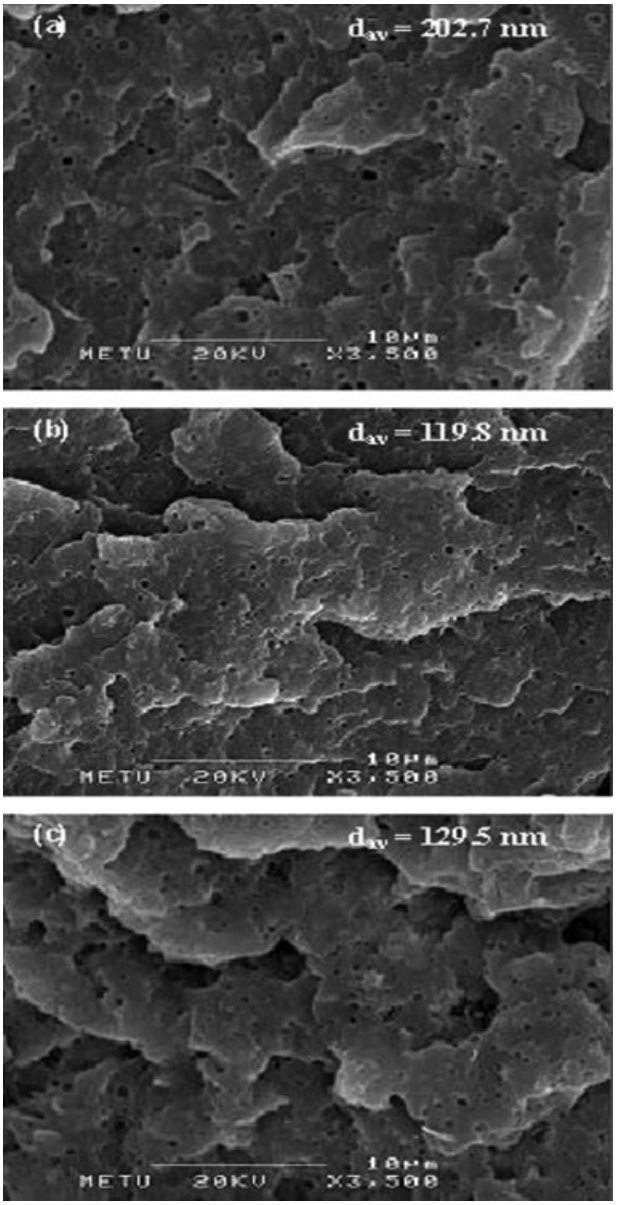

Figure 7 SEM micrographs of PA 66-Cloisite® 15A-Lotader® AX8840 mixing sequences: (a) CI-P (3500×); (b) PC-I (3500×); (c) PI-C (3500×).

Domain size distribution and interdomain distance are also highly dependent upon the modulus of the matrix, matrix modulus/elastomer modulus ratio, interfacial adhesion, shear stress, the melt viscosity and melt elasticity ratios of the components, and interface mobility.[22]

The domain sizes of All-S mixing sequences of Cloisite® 15A nanocomposites were found to be smaller than Cloisite® 25A-(All-S) nanocomposites, whereas the smallest domain sizes belong to Cloisite® 30B-(All-S) nanocomposites. Lack of elastomer domains at an optimum size and interdomain distance facilitate the crack propagation since elastomer domains can act as stress concentrators resulting from their cavitation effect. The profound effect of the degree of organoclay dispersion on the domain size distribution of the elastomeric phase cannot be ignored hence the agglomeration of elastomer domains is suppressed by the exfoliated clay platelets.[21] This verifies the decrease in the domain sizes of Cloisite® 15A that displayed a partially exfoliated structure. Incorporation of the organoclay into polyamide 66-8840 blend generally decreased the elastomeric domain sizes in All-S blending sequences. Elastomeric domain sizes of All-S mixing sequence are not influenced by the addition order since all the constituents were compounded together, thus a comparison can be made between the domain sizes of

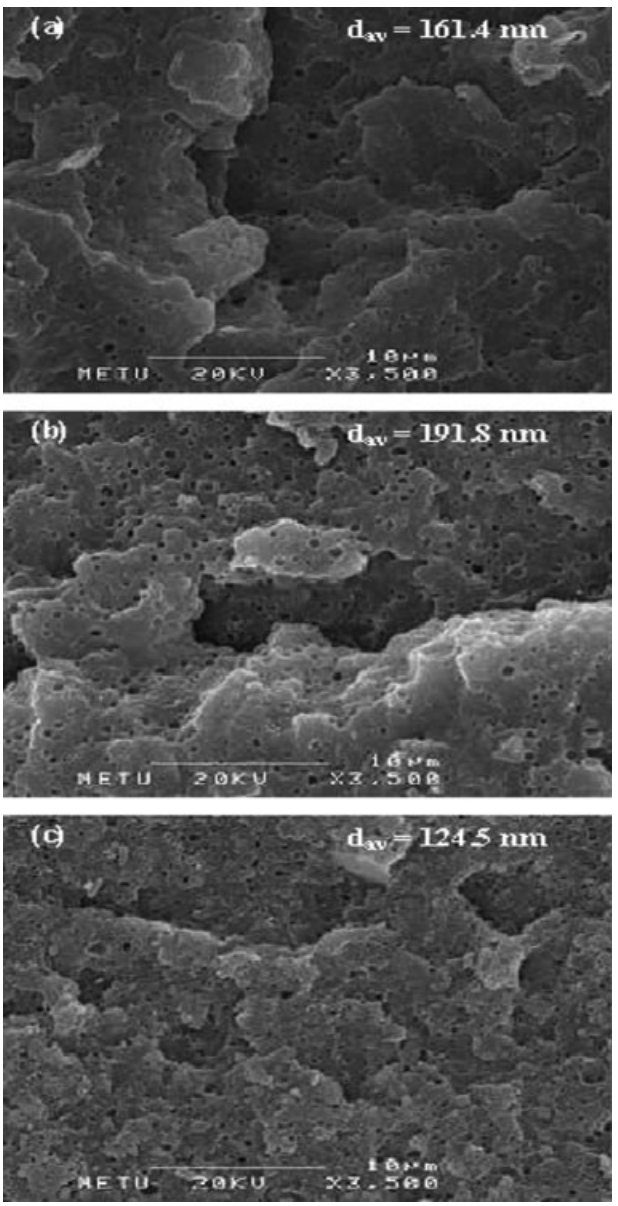

Figure 8 SEM micrographs of PA 66-Cloisite® 25A-Lotader® AX8840 mixing sequences: (a) CI-P (3500×); (b) PC-I (3500×); (c) PI-C (3500×).

the blend and All-S mixing sequences. Although the presence of the organoclays decreased the domain sizes with respect to the blend, the slight increase in the domain sizes of All-S nanocomposites containing Cloisite® 25A can be attributed to the possible interaction between the impact modifier and the organoclay or the presence of the organoclay in the impact modifier which can prevent the decrease in their sizes.[20]

Addition order of the components is one of the primary factors which result in changes in the domain sizes of the elastomer. Increased shear intensity, melt viscosity, and interfacial adhesion between the components decrease the domain sizes dramatically. The domain sizes of PI-C mixing sequences are expected to be similar with the domain sizes of All-S mixing sequences. However, they are close to the domain sizes of CI-P and PC-I mixing sequences. This can arise from the insufficient shear intensity since organoclay was extruded with the polymer matrix only once in PI-C blending sequence. Despite being extruded twice, the domain sizes of the elastomer are similar with the others for CI-P mixing sequence, too. Some of the organoclay may have been retained in the elastomer domains or the interactions between the elastomer and the clay may have prevented a substantial decrease in the domain sizes. Elastomeric phase was extruded only once in PC-I mixing sequence, thus the elastomer agglomerations cannot be broken down into smaller elastomeric domains in one extrusion step. Therefore, it is expected to obtain an increase in the domain sizes of PC-I blending sequences compared to All-S mixing sequences.

The reduction obtained in the domain sizes of CI-P, PC-I, and PI-C mixing sequences is inferior to the reduction obtained in All-S mixing sequences. Therefore, it is more favorable to compound all the constituents simultaneously considering the interactions occurring between them and the shear intensity applied on all of them in both of the extrusion steps.

MFI analysis

Melt flow that is inversely proportional to the melt viscosity is affected tremendously by the processing techniques, molecular weight of the polymer matrix, and the type of the additives. MFI values are given in Table II.

MFI values of pure polyamide 66 and the one that was twice extruded are almost the same indicating that degradation of the polymer during extrusion is negligible. It is a well-known fact that fillers resist flow especially at low shear rates and cause an increase in the melt viscosity. Size, shape, and concentration of the filler induce changes in the MFI. However, MFI values increased for the binary nanocomposites in contrast to the behavior exhibited by conventional composites. It can be ascribed to the slip between the polymer matrix and the dispersed clay platelets since the change in the melt viscosity of extruded polyamide 66 is ignorable in comparison with neat polyamide 66.[32,33] MFI values of the nanocomposites and polymer matrix are relatively high compared to the blend since the elastomeric material has higher viscosity compared to the polymer matrix. Addition of the organoclay into the blend did not cause large variations in the melt viscosity.

TABLE II
MFI Values of Polyamide 66 Nanocomposites

Components	T_m (°C)	Crystallinity (%)
PA 66	262.96	25.6
PA 66-8840	261.92	22.9
PA 66 binary nanocomposites		
PA 66-15A	263.41	24.7
PA 66-25A	261.78	23.5
PA 66-30B	261.51	23.9
PA 66 ternary nanocomposites		
(PA 66-15A-8840)-(All-S)	262.16	23.7
(PA 66-25A-8840)-(All-S)	262.74	21.7
(PA 66-30B-8840)-(All-S)	262.14	23.5
Mixing sequences of PA 66 ternary nanocomposites		
(15A/8840)-PA 66-(CI-P)	262.33	22.3
(PA 66/15A)-8840-(PC-I)	262.00	26.1
(PA 66/8840)-15A-(PI-C)	261.56	22.3
(25A/8840)-PA 66-(CI-P)	262.08	24.0
(PA 66/25A)-8840-(PC-I)	263.03	27.0
(PA 66/8840)-25A-(PI-C)	261.82	22.9

Melt viscosity is directly related with the degree of organoclay dispersion since the shear intensity applied on the clay platelets increases proportionally with the melt viscosity and it becomes easier to tear the clay platelets apart. Hereby, the clay platelets were dispersed more homogeneously by the help of the increased melt viscosity in ternary nanocomposites as it can also be seen in XRD patterns.

MFI values of CI-P and PI-C mixing sequences were found to be lower than PC-I mixing sequence. However, melt viscosity was not much useful in delamination of the organoclay for the nanocomposites of PI-C mixing sequences. This can be attributed to the aforementioned reasons arising from extrusion of the impact modifier and polymer without the organoclay in the first extrusion step.

DSC analysis

Crystallinity of the polyamide 66 matrix in the nanocomposites and in the blend is given in Table III. Crystallinity is correlated with the enhancements in the mechanical properties.

Crystallization begins as soon as the crystallization temperature is reached in nanocomposites since heterogeneous nucleation occurs during the crystalliza-

TABLE III
Crystallinity and Melting Point of Polyamide 66 Nanocomposites

Components	Tensile strength (MPa)	Young's modulus (MPa)	Elongation at break (%)	Impact strength (kJ/m^2)
PA 66	78.1 ± 3.6	2266 ± 74	37.3 ± 6.1	4.4 ± 0.4
PA 66-8840	66.8 ± 0.3	1705 ± 38	52.1 ± 3.9	6.7 ± 0.5
PA 66 binary nanocomposites				
PA 66-15A	82.8 ± 0.3	2533 ± 35	17.0 ± 2.6	4.0 ± 0.3
PA 66-25A	81.7 ± 0.4	2434 ± 78	18.0 ± 1.8	3.5 ± 0.3
PA 66-30B	81.2 ± 0.5	2406 ± 90	25.3 ± 6.8	3.8 ± 0.6
PA 66 ternary nanocomposites				
(PA 66-15A-8840)-(All-S)	70.0 ± 0.1	1728 ± 34	43.5 ± 7.6	6.4 ± 0.8
(PA 66-25A-8840)-(All-S)	69.0 ± 0.6	1782 ± 139	39.3 ± 10.7	6.2 ± 1.2
(PA 66-30B-8840)-(All-S)	69.4 ± 0.2	1748 ± 28	41.8 ± 2.3	5.9 ± 0.3
Mixing sequences of PA 66 ternary nanocomposites				
(15A/8840)-PA 66-(CI-P)	64.6 ± 0.8	1721 ± 50	46.9 ± 3.5	5.6 ± 0.5
(PA 66/15A)-8840-(PC-I)	67.8 ± 3.7	1742 ± 22	48.8 ± 5.2	6.1 ± 0.7
(PA 66/8840)-15A-(PI-C)	62.3 ± 0.8	1690 ± 35	28.1 ± 9.0	4.5 ± 1.0
(25A/8840)-PA 66-(CI-P)	63.4 ± 0.5	1716 ± 74	49.8 ± 1.8	4.6 ± 1.5
(PA 66/25A)-8840-(PC-I)	65.7 ± 3.7	1722 ± 74	32.4 ± 12.8	5.1 ± 1.0
(PA 66/8840)-25A-(PI-C)	64.3 ± 0.9	1720 ± 34	26.6 ± 5.2	4.2 ± 0.8

tion process. Montmorillonite layers serve as active sites for nucleation and the temperature to reach maximum crystallization rate increases as a result.[34]

The function of the organoclay in nanocomposites is to decrease the crystallite size and increase the crystallization temperature.[35] Dispersion of the silicate layer, processing factors, and the resultant conformation of the polymer chains determines the relation between the structure and the property of the nanocomposites.[20] It seems that crystallinity does not significantly depend on either the elastomer content or the organoclay content, thus crystallinity did not significantly contribute to the changes in the mechanical properties. It is the type of the components and their addition order what affected the properties of the nanocomposites.

Mechanical properties

Tensile test results are evaluated using the data displayed in Figures 9–11. The tensile and impact results are also summarized in Table IV. The interfacial adhesion between polyamide 66 and organoclay, the large contact area created by the high aspect ratio of the clay, and uniform distribution of the clay platelets are all pertinent with the increases in the tensile strength and modulus of the nanocomposites. However, the reduced tie chain amount between the crystalline areas impedes stress transfer through the sample leading to early failure of the material. The energy absorption occurring during the crack formation is increased by incorporation of elastomeric materials which enhance the interaction between organoclay and polymer matrix. Improvements in the tensile strength and modulus surmount the decrease in ductility in binary nanocomposites since inorganic silicate platelets cannot be strained by external stresses.[22] The highest increase in the tensile test results is observed for Cloisite® 15A nanocomposites, followed by Cloisite® 25A and Cloisite® 30B nanocomposites just like the dispersion level in XRD patterns. Nevertheless, the differences between the tensile strength and modulus of the nanocomposites are slight. This can be associated with the intercalated regions present in the morphological structure of all the nanocomposites. The variations in the tensile test results of the other mixing sequences are also susceptible to the dispersion of the organoclay in the polymer matrix. All-S mixing sequences which generally exhibit the highest improvements in the

TABLE IV
Tensile and Impact Rest Results of Polyamide 66 Nanocomposites

Components	MFI (g/10 min)
PA 66 (not extruded)	16.4 ± 1.6
PA 66 (twice extruded)	16.3 ± 1.0
Lotader® AX8840	5.4 ± 0.2
PA 66-8840	11.6 ± 3.0
PA 66 binary nanocomposites	
PA 66-15A	17.7 ± 2.6
PA 66-25A	18.7 ± 1.4
PA 66-30B	16.6 ± 0.4
PA 66 ternary nanocomposites	
(PA 66-15A-8840)-(All-S)	8.1 ± 0.2
(PA 66-25A-8840)-(All-S)	8.5 ± 0.3
(PA 66-30B-8840)-(All-S)	9.4 ± 0.7
Mixing sequences of PA 66 ternary nanocomposites	
(15A/8840)-PA 66-(CI-P)	11.5 ± 0.9
(PA 66/15A)-8840-(PC-I)	13.2 ± 0.7
(PA 66/8840)-15A-(PI-C)	12.6 ± 1.3
(25A/8840)-PA 66-(CI-P)	11.9 ± 0.5
(PA 66/25A)-8840-(PC-I)	12.3 ± 0.7
(PA 66/8840)-25A-(PI-C)	11.8 ± 0.5

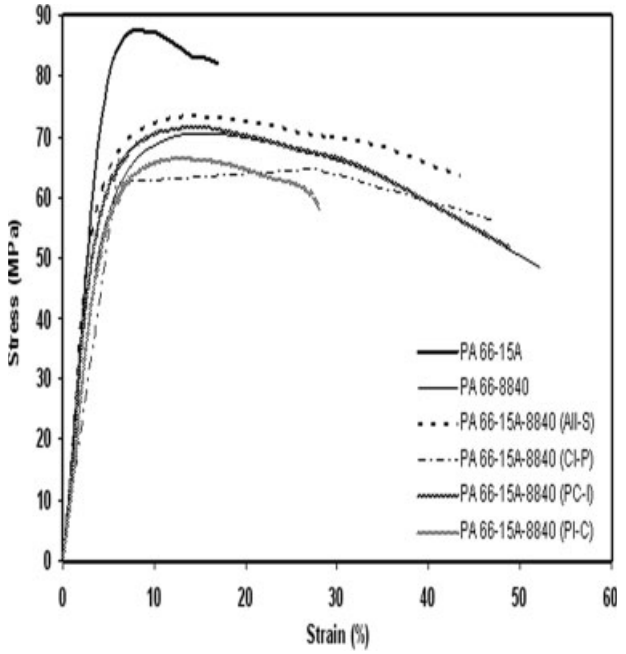

Figure 9 Stress–strain curves of PA 66-Cloisite® 15A-Lotader® AX8840 mixing sequences.

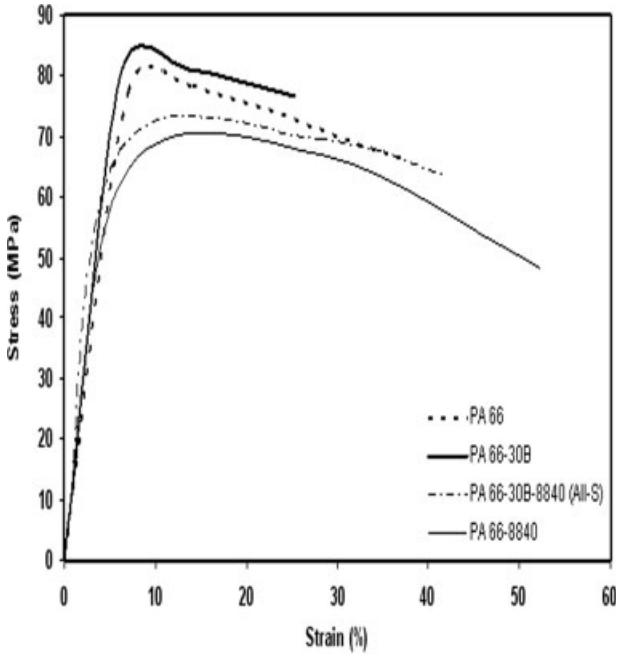

Figure 11 Stress–strain curves of PA 66-Cloisite® 30B nanocomposites.

tensile test results are followed by PC-I, CI-P, and PI-C mixing sequences. This can also be seen obviously from the increase in the mechanical properties of All-S mixing sequence compared to the blend. (PA 66-15A-8840)-(All-S) has the mostly improved mechanical properties among all the mixing sequences. In PI-C mixing sequences, the organoclay dispersion is not as uniform as the other mixing sequences and the elastomeric domains are rather large resulting from extrusion of the organoclay with polymer-impact modifier combination in only one extrusion step. As long as the organoclay is not distributed uniformly in the matrix, formation of elastomer agglomerations cannot be prevented since organoclay can immobilize the interface, and function as barriers preventing the coalescence of the elastomer domains.[21] On the other hand, some of the organoclay platelets may be present in the elastomeric phase rather than be dispersed in the polymer matrix in CI-P mixing sequences. All these factors can retard the improvements in the mechanical properties for PI-C and CI-P mixing sequences. The domain sizes of PI-C, CI-P, and PC-I mixing sequences are also quite close to each other. Higher viscosity of PI-C and CI-P mixing sequence enhanced neither the organoclay dispersion in the polymer matrix nor the mechanical properties in comparison with PC-I mixing sequence. It may be better to increase the organoclay content further in all the ternary nanocomposites to obtain higher increase in the strength with respect to the polymer matrix.

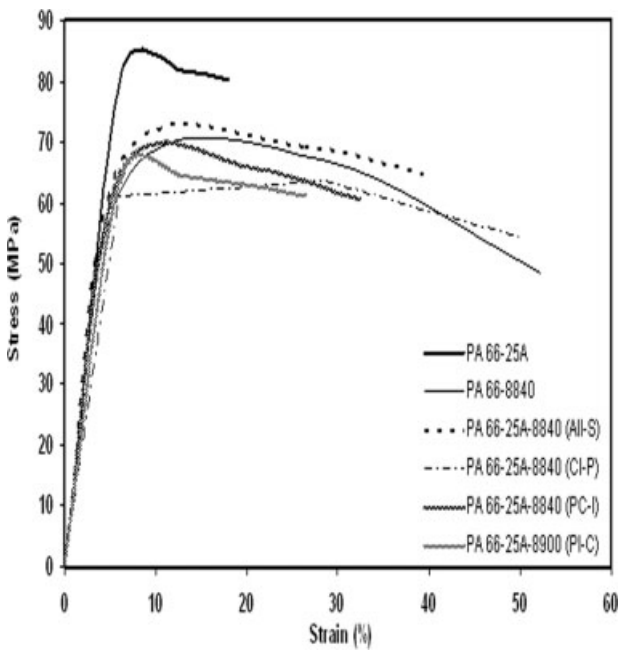

Figure 10 Stress–strain curves of PA 66-Cloisite® 25A-Lotader® AX8840 mixing sequences.

Toughness is dependent upon a variety of factors including the modulus ratio of the elastomeric phase and the polymer matrix, uniform dispersion of the organoclay, stability of the interface, interfacial adhesion between the components, modulus of the matrix, domain size distribution of the elastomer, and interdomain distance. Impact strength was found to be higher for Cloisite® 15A and Cloisite® 25A nanocomposites compared to Cloisite® 30B nanocomposites.

The increase in the impact strength of CI-P, PC-I, and PI-C, mixing sequences is similar to the increase in the tensile test results. The impact strength values of the blend and the ternary nanocomposites especially All-S mixing sequences are close to each other. However, mixing sequence plays an important role on the mechanical properties. The mechanical properties of (25A/8840)-PA 66-(CI-P) mixing sequence are not as improved as the mechanical properties of All-S mixing sequences besides its exfoliated structure. It can be asserted that homogeneous dispersion of the organoclay promotes the enhancements in both the impact strength and the tensile strength test results. Yet, it is better to compound all of the constituents simultaneously as in All-S mixing sequences since the same shear intensity is applied on all of the components and the interactions taking place between them are not minimized to a single extrusion step.

CONCLUSIONS

XRD analysis show that the best organoclay dispersion is obtained in Cloisite® 15A nanocomposites followed by Cloisite® 25A and Cloisite® 30B nanocomposites. Melt compounding of all the components twice aided dispersion of the organoclays in the polymer matrix. The interactions of the polar groups of the organic modifier with the polar groups in its structure and with the oxygen atom on the clay surface may have resulted in a high packing density, and prevent diffusion of the polymer chains in the intergallery of the clay for Cloisite® 30B. The insufficient shear stress applied in a single extrusion step is considered as the reason hindering dispersion of the organoclay in PI-C mixing sequence besides the increases in its melt viscosity. Variations in the dispersion levels of the organoclay in mixing sequences stem from the differences in the addition orders since each component is not subjected to the same shear intensity.

SEM analyses also verify that organoclay delamination causes a decrease in the domain sizes. It is determined that the domain sizes and the interdomain distance have to be within a specific range to prevent the crack propagation. The highest toughness results belong to Cloisite® 15A nanocomposites. On the other hand, the lowest toughness increase is observed in Cloisite® 30B nanocomposites whose domain sizes are really small and interparticulate distance is really large. The domain sizes of PI-C mixing sequence was found to be relatively large with respect to All-S mixing sequence hence it was extruded without the organoclay in the first extrusion step and the barrier effect of the delaminated clay platelets to break up the elastomer agglomerates was eliminated. Although the impact modifier was only extruded once in PC-I mixing sequence, the domain sizes of CI-P mixing sequence were also found to be close to it. This can arise from the affinity of the organoclay to the elastomeric phase and the presence of some organoclay in the elastomeric domains. The increase in both the tensile and the impact test results are in accordance with the degree of organoclay and elastomeric domain dispersion. All-S mixing sequences has improved mechanical properties with respect to the blend. (PA 66-15A-8840)-(All-S) exhibits the most improved properties among all the mixing sequences. Although the organoclay was completely exfoliated in (25A/8840)-PA 66-(CI-P) mixing sequence, variation in the addition order of the components eliminated the enhancements in the mechanical properties. Increase in the amount of organoclay in the ternary composites can result in a higher increase in the strength and modulus values since significant increases could not be obtained when the organoclay content is kept at 2 wt %.

MFI results show that decreased MFI values of the ternary nanocomposites aid dispersion of the organoclay. However, the melt viscosity of the binary nanocomposites decreased with respect to the polymer matrix although there is not a reduction in the molecular weight of polyamide 66. It is attributed to the slip effect between the oriented clay layers and the polymer matrix.

Nearly no change is observed in the crystallinity of polyamide 66 in the blend or nanocomposites. Crystallinity changes did not significantly contribute to the variations in the properties of polyamide 66 nanocomposites.

References

1. Alexandre, M.; Dubois, P. Mater Sci Eng 2000, 28, 1.
2. Yu, Z. Z.; Yang, M.; Zhang, Q.; Zhao, C.; Mai, Y. W. J Polym Sci Part B: Polym Phys 2003, 41, 1234.
3. Fornes, T. D.; Yoon, P. J.; Keskkula, H.; Paul, D. R. Polymer 2001, 42, 9929.
4. Kelnar, I.; Kotek, J.; Kaprálková, L.; Munteanu, B. S. J Appl Polym Sci 2005, 96, 288.
5. Tomova, D.; Radusch, H. J Polym Adv Technol 2003, 14, 19.
6. Pinnavaia, T. J.; Beall, G. W. Polymer-Clay Nanocomposites; Wiley: Chichester, 2006.
7. Yano, K.; Usuki, A.; Okada, A.; Kurauchi, T.; Kamigaito, O. J Polym Sci Part A: Polym Chem 1993, 31, 2493.
8. Yano, K.; Usuki, A.; Okada, A. J Polym Sci Part A: Polym Chem 1997, 35, 2289.
9. Gilman, J. W.; Jackson, C. L.; Morgan, A. B.; Harris, R., Jr.; Manias, E.; Giannelis, E. P.; Wuthenow, M.; Hilton, D.; Philips, S. H. Chem Mater 2000, 12, 1866.
10. Gilman, J. W.; Kashiwagi, T.; Lichtenhan, J. D. SAMPE J 1999, 33, 40.
11. Gilman, J. W. Appl Clay Sci 1999, 15, 31.
12. Giannelis, E. P. Appl Organomet Chem 1998, 12, 675.
13. Kojima, Y.; Usuki, A.; Kawasumi, M.; Okada, A.; Kurauchi, T.; Kamigaito, O. J Polym Sci Part A: Polym Chem 1993, 31, 983.

14. Kojima, Y.; Usuki, A.; Kawasumi, M.; Okada, A.; Kurauchi, T.; Kamigaito, O. J Polym Sci Part A: Polym Chem 1993, 31, 1755.
15. Kroschwitz, J. I.; Mark, H. F. Encyclopedia of Polymer Science and Technology, 3rd ed.; Wiley Interscience: Hoboken, NJ, 2003.
16. Avella, M.; Bondioli, F.; Cannillo, V.; Di Pace, E.; Errico, M. E.; Ferrari, A. M.; Focher, B.; Malinconico, M. Compos Sci Technol 2006, 66, 886.
17. Ray, S. S.; Okamoto, M. Prog Polym Sci 2003, 28, 1539.
18. Dennis, H. R.; Hunter, D. L.; Chang, D.; Kim, S.; White, J. L.; Cho, J. W.; Paul, D. R. Polymer 2001, 42, 9513.
19. Fornes, T. D.; Yoon, P. J.; Hunter, D. L.; Keskkula, H.; Paul, D. R. Polymer 2002, 43, 5915.
20. Dasari, A.; Yu, Z. Z.; Yang, M.; Zhang, Q. X.; Xie, X. X.; Mai, Y. W. Compos Sci Technol 2006, 66, 3097.
21. Hassan, A.; Othman, N.; Wahit, M. U.; Wei, L. J.; Rahmat, A. R.; Ishak, Z. A. M. Macromol Symp 2006, 239, 182.
22. Contreras, V.; Cafiero, M.; Da Silva, S.; Rosales, C.; Perera, R.; Matos, M. Polym Eng Sci 2006, 46, 1111.
23. Kohan, M. I. Nylon Plastics; Wiley: New York, 1973.
24. Shen, L.; Phang, I. Y.; Chen, L.; Liu, T.; Zeng, K. Polymer 2004, 45, 3341.
25. Xu, W.; Liang, G.; Wang, W.; Tang, S.; He, P.; Pan, W. P. J Appl Polym Sci 2003, 88, 3225.
26. Gonzáles, I.; Eguiazábal, J. I.; Nazábal, J. Compos Sci Technol 2006, 66, 1833.
27. Mehrabzadeh, M.; Kamal, M. Polym Eng Sci 2004, 44, 1151.
28. Chang, J.; An, Y. U. J Polym Sci Part B: Polym Phys 2002, 40, 670.
29. Paul, D. R.; Zeng, Q. H.; Yu, A. B.; Lu, G. Q. J Colloid Interface Sci 2005, 292, 462.
30. Sikdar, D.; Katti, D. R.; Katti, K. S.; Bhowmik R. Polymer 2006, 47, 5196.
31. Tedesco, A.; Krey, P. F.; Barbosa, R. V.; Mauler, R. S. Polymer Int 2001, 51, 105.
32. Cho, J. W.; Paul, D. R. Polymer 2001, 42, 1083.
33. Gonzáles, I.; Eguiazábal, J. I.; Nazábal, J. Polymer 2005, 46, 2978.
34. Zhang, Q. X.; Yu, Z. Z.; Yang, M.; Ma, J.; Mai, Y. W. J Polym Sci Part B: Polym Phys 2003, 41, 2861.
35. Liu, X.; Wu, Q.; Berglund, L. A. Polymer 2002, 43, 4967.